

Supporting Information

Electrochemical Immunosensor for Simultaneous point-of-care Cancer markers Based on Host-Guest Inclusion of β -cyclodextrin-Graphene oxide

Taotao Feng,^a Xiuwen Qiao*,^a Haining Wang,^a Zhao Sun,^a Yu Qi*,^a Chenglin Hong*^{a, b}

^a School of Chemistry and Chemical Engineering, Shihezi University, Shihezi 832003 PR China

^b Key Laboratory for Green Processing of Chemical Engineering of Xinjiang Bingtuan, Engineering Research Center of Materials-Oriented Chemical Engineering of Xinjiang Production and Construction Corps, Key Laboratory of Materials-Oriented Chemical Engineering of Xinjiang Uygur Autonomous Region, Shihezi 832003 PR China

*Corresponding author:

Tel.: +86-18097586568; Fax: +86-993-2057270;

E-mail: hcl_tea@shzu.edu.cn (Chenglin Hong). qy01_tea@shzu.edu.cn (Yu Qi).

qxw_tea@shzu.edu.cn (Xiuwen Qiao).

1.1 Material and Reagents

Ferrocenecarboxylic acid (Fc-COOH), gold chloride tetrahydrate ($\text{HAuCl}_4 \cdot 4\text{H}_2\text{O}$), graphite powders, β -cyclodextrin (β -CD), **potassium permanganate** (KMnO_4), *N*-Hydroxysuccinimide (NHS), 1-(3-Dimethylaminopropyl)-3-ethylcarbodiimide hydrochloride (EDC) and concentrated sulphuric acid (H_2SO_4) were from **Aladdin** (Shanghai, China). **Ammonia** ($\text{NH}_3 \cdot \text{H}_2\text{O}$), Hydroxylamine hydrochloride ($\text{NH}_2\text{OH} \cdot \text{HCl}$) were purchased from **Guangfu** Institute of Fine Chemicals (**Tianjin, China**). Bovine serum albumin (BSA) was supplied by Alfa Aesar (Tianjin, China). CEA antigens, alpha fetoprotein (AFP) antigens and anti-CEA antibodies were purchased from Biocell Biotechnology Co., Ltd. (**Zhengzhou, China**), Sodium dodecyl sulphate (SDS) was from Huihuang Chemical Reagent (**Yixing, China**). The supporting electrolyte was 0.1 M PBS containing 0.1 M KCl. All reagents were of analytical-reagent grade.

1.2 Apparatus

Electrochemical experiments (CV, DPV and EIS) were carried out on a Potentiostat/Galvanostat Model 283 Electrochemical analyzer with three-electrode system (Mattson, America). Transmission electron microscope (TEM) was made on a Hitachi H-600 (Hitachi, Japan). X-ray powder diffraction (XRD) was performed on a Bruker D8 advanced (Bruker, Germany). Fourier-transform infrared (FT-IR) was determined using a Nicolet Avatar 360 FT-IR spectrometer (Thermo Nicolet Corporation, America). KQ-250B ultrasonic cleaning instrument (Kunshan Ultrasonic Instrument, China), HH-S digital thermostat water bath (Jiangsu Jintan Medical Instrument, China), GZX-9140 MBE-type electric oven blast (Shanghai Jinghong Experimental Equipment, China) was used in the work.

1.3 Synthesis of AuNPs-GO

Graphene oxide was synthesized according to a modified Hummer's method.¹ The GO-AuNPs was synthesized according to literature with a little modification.^{2,3} Briefly, 5 mg of GO was dispersed into 10 mL of distilled water, which was sonicated for 30 min to obtain a yellow-brown aqueous solution. Then, 0.5 mL of HAuCl₄ (1.0 wt %) and 0.2 g of NaOH were quickly added, and then the mixed solution was sonicated for another 2 h. Finally, the mixture was centrifuged and washed to remove the remaining reagents and re-dispersed in 5 mL of distilled water.

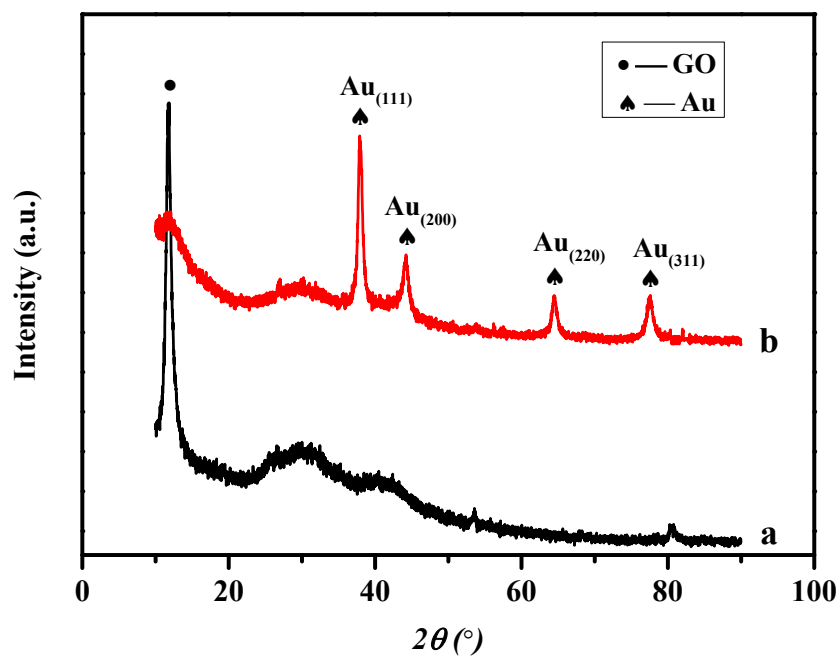


Fig.S1 XRD of GO (a) and GO-AuNPs (b)

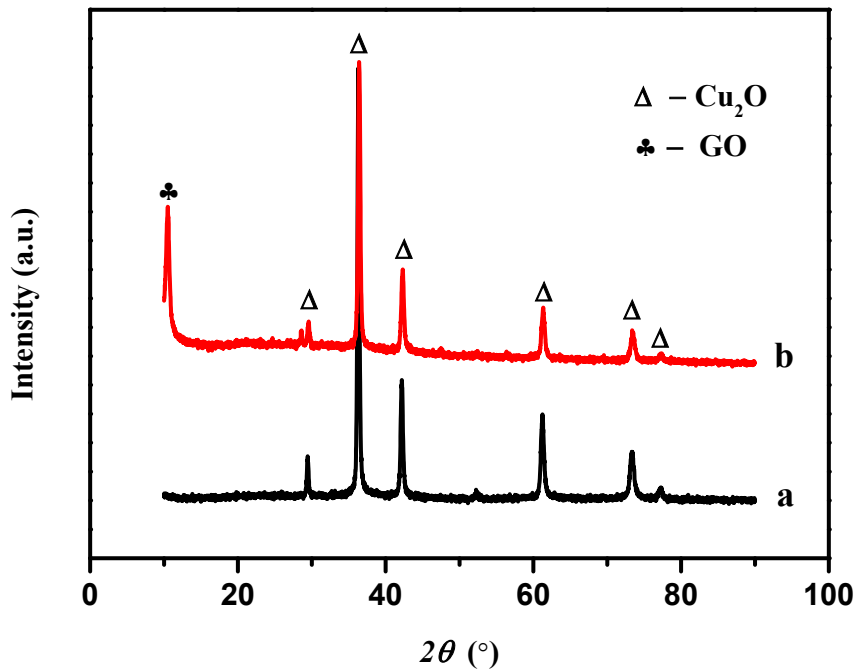
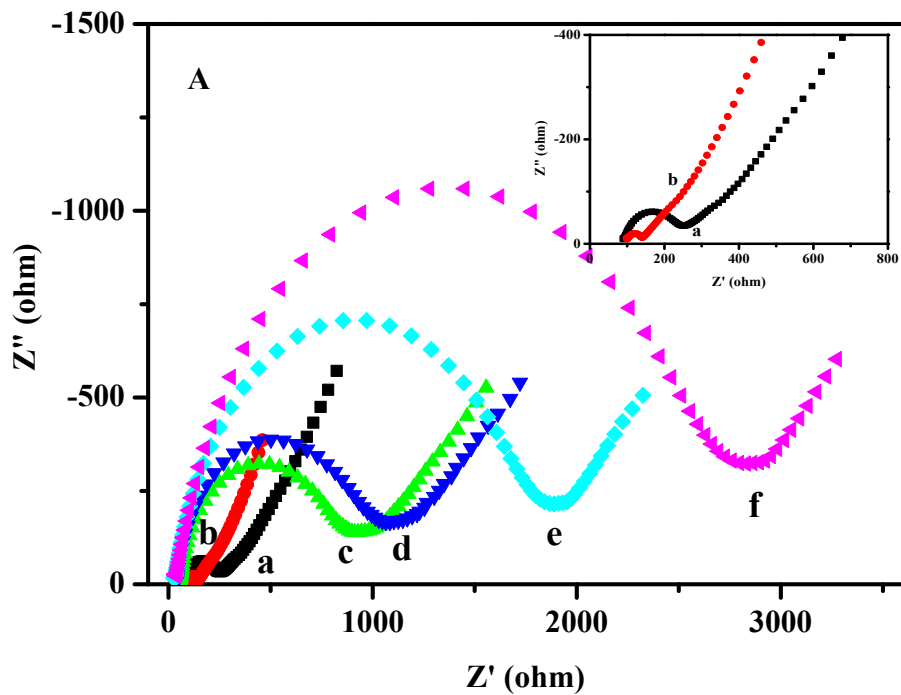


Fig.S2 XRD of Cu_2O (a) and $\text{Cu}_2\text{O-GO}$ (b)

The GO and GO-AuNPs were characterized by XRD. As shown in Fig.S1, a prominent diffraction peak of GO at 11° was to be seen (curve a). Diffraction peaks

located at 36.2° , 43.1° , 66.0° and 78.0° , which should be attributed to the diffraction of (111), (200), (220) and (311) planes of AuNPs (curve b). This result indicates that AuNPs was **successful anchored** on the surfaces of GO.

The GO and Cu_2O -GO **were also characterized** by XRD. As shown in Fig. S2, the pattern of GO reveals an intense sharp peak at 10.6° , corresponding to the (002) inters planar spacing. The strong diffraction peaks at 29.4° , 36.4° , 42.2° , 61.3° , 73.4° and 77.2° were indexed as (110), (111), (200), (220), (311) and (222) crystal planes reflections (curve a) of pure Cu_2O with cubic phase (JCPDS file No. 78-2076). It also should be noted that no diffraction peaks from impurities were observed, indicating the pure cuprous Cu_2O phase of the as-synthesized products.



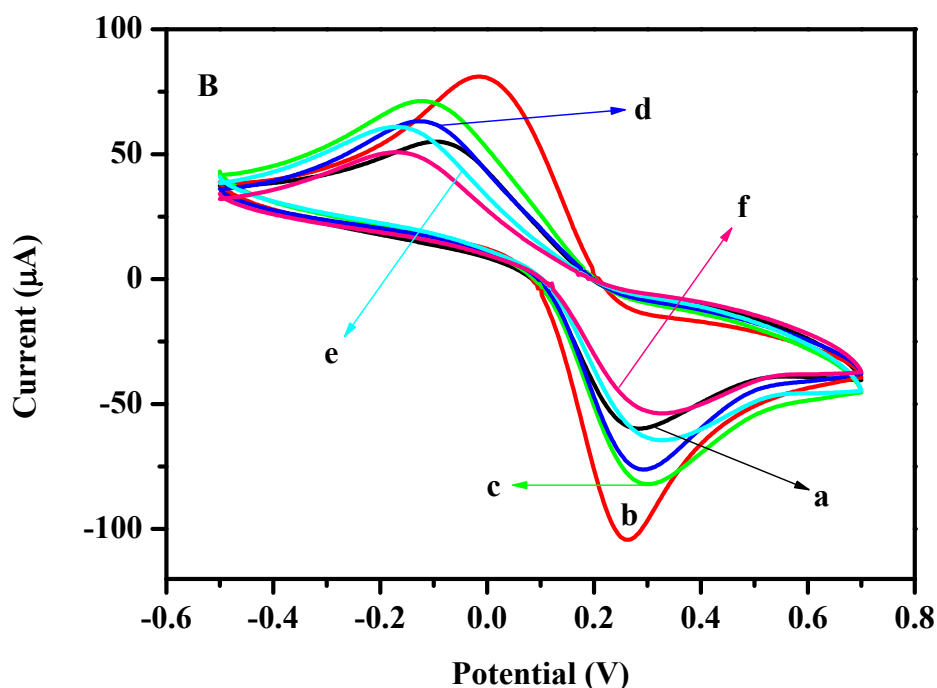


Fig.S3 EIS (A) and CVs (B) of bare GCE (curve a), GO-AuNPs/GCE (curve b), Ab₁/GO-AuNPs/GCE (curve c), BSA/Ab₁/GO-AuNPs/GCE (curve d), antigen/BSA/Ab₁/GO-AuNPs/GCE (curve e), bioconjugates-Ab₂/antigen/BSA/Ab₁/GO-AuNPs/GCE (curve f) modified electrode in 0.1 M PBS (pH 7.4) solution containing 0.1 M KCl and 5 mM [Fe(CN)₆]^{3-/4-}. Scan rate: 50 mV·s⁻¹. Frequency varies from 0.01 to 10⁵ Hz.

Cyclic voltammetry (CV) and electrochemical impedance spectroscopy (EIS) were used to monitor the stepwise construction process of the electrochemical immunosensor in 0.1 M PBS (pH 7.4) solution containing 0.1 M KCl and 5 mM [Fe(CN)₆]^{3-/4-}. As shown in Fig. S3B, a pair of distinct redox peaks were observed at a bare GCE electrode (curve a) that was attributed to a one-electron electrochemical process of [Fe(CN)₆]^{3-/4-} probe. The peak current increased sharply (curve b) when the bare GCE electrode was modified with GO-AuNPs, indicating that the GO-AuNPs could accelerate the electron transfer on the surface of modified GCE electrode. However, after the GO-AuNPs/GCE electrode was incubated in primary anti-CEA and anti-AFP, the peak currents decreased significantly (curve c). The reason was that under AuNPs assistance, a large of primary antibodies without deactivation was immobilized on the surface of GCE/GO-AuNPs electrode. The protein formed a block layer on the

surface of modified electrode to block the electron transfer of $[\text{Fe}(\text{CN})_6]^{3-/4-}$ probe. Next, BSA was used to block remaining active sites of the modified electrode surface, the peak current further decreased (curve d) because of BSA could blocked the electron transfer. Then, the modified electrode was incubated in CEA and AFP, the peak current decreased (curve e). The reason was that the protein prevents electron transfer. When the modified electrode was incubated in the mixture of Cu_2O -GO-anti-AFP and GO-CD-Fc-anti-CEA, the peak current decreased (curve f), due to antigen and antibody specific binding formation immune-complexes and further blocks the electron transfer.

Electrochemical impedance spectroscopy (EIS) was also an important tool for monitoring the impedance changes of modified electrodes surface. To further monitor the surface conditions of the modified electrodes, EIS has been employed to characterize the surface properties of different modified electrodes. The electrochemical impedance spectra consist of a semicircle at high frequencies corresponding to the electron transfer limiting process, and a line at low frequencies resulting from the diffusion limiting step of the electrochemical process. The diameter of the semicircle corresponds to the electron-transfer resistance (R_{et}), which could be estimated from the diameter of the semicircle. As shown in Fig. S3A, the bare GCE electrode have a small semicircle (curve a). The resistance decreased (curve b) when GO-AuNPs was modified on the surface of GCE electrode because GO-AuNPs have good conductivity and could accelerate the electron transfer. After primary anti-CEA and anti-AFP was immobilized on the surface of GCE/GO-AuNPs electrode, the resistance increased dramatically (curve c). The result was consistent with the fact that the hydrophobic layer of proteins insulates the conductive support and hinders the electron transfer. The resistance increased (curve d) when BSA was used to block the remaining active sites. Then, the electrode was incubated in CEA and AFP, the resistance increased (curve e). Finally, the resistance further increased (curve f) when Cu_2O -GO-CD-anti-AFP and GO-CD-Fc-anti-CEA was used specific bio-recognition AFP and CEA of the GCE/GO-AuNPs/anti-AFP or -CEA surface because the antigen-antibody immune-complexes could resist the electron transfer kinetics at the

electrode interface. The results which were good consistent with those obtained through CV measurements demonstrated the successful fabricated process of the electrochemical immunosensor.

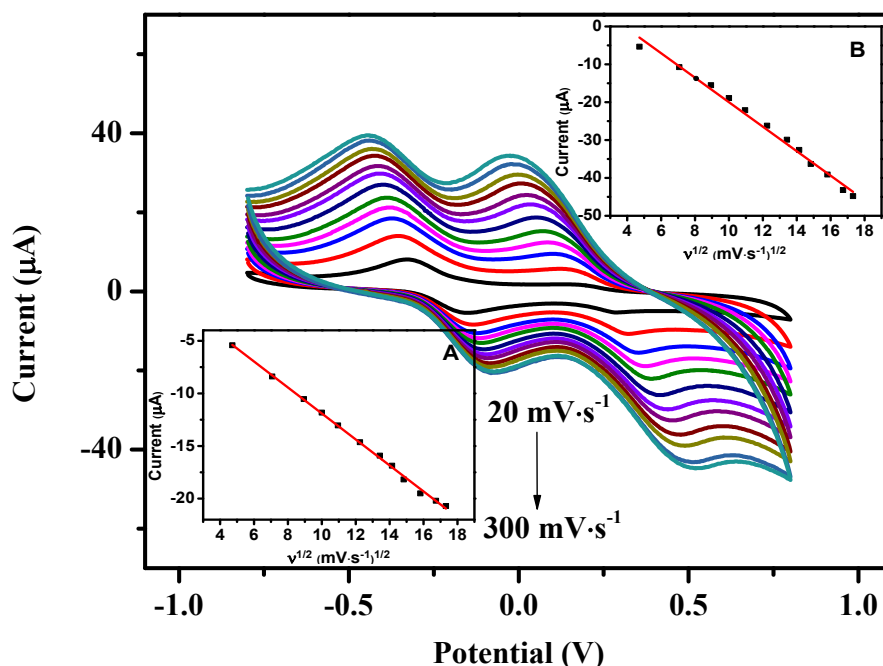


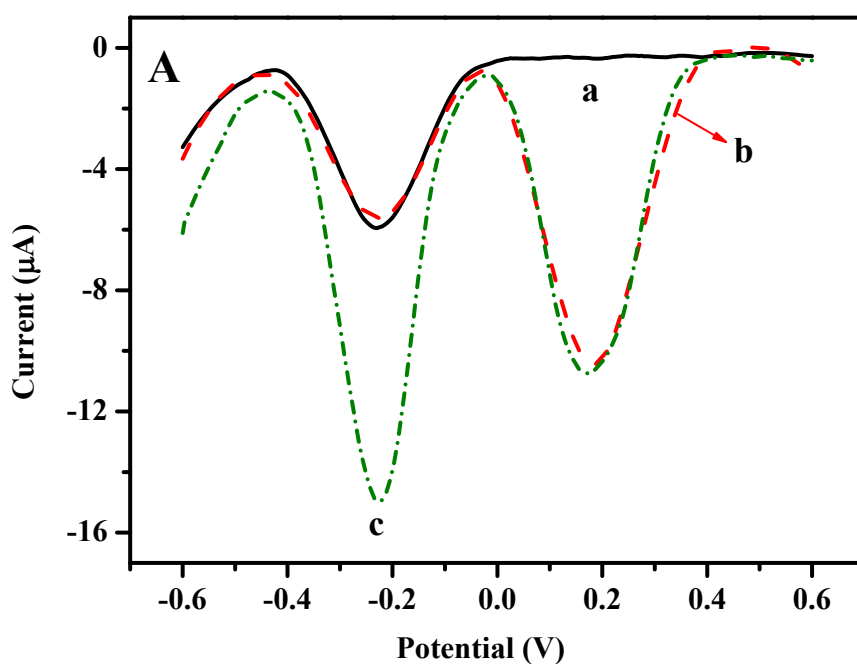
Fig. S4 CVs of electrochemical immunosensor at different scan rate of 20, 50, 80, 100, 120, 150, 180, 200, 220, 250, 280, 300 $\text{mV}\cdot\text{s}^{-1}$ in 0.1 M PBS (pH 7.4) solution containing 0.1 M KCl under optimal conditions. Insets showed the peak current of (A) AFP and (B) CEA proportional to the square root of scan rate. Scan rate: $50 \text{ mV}\cdot\text{s}^{-1}$

1.4 Evaluation of cross-reactivity and cross-talk

An ideal simultaneous detection electrochemical immunosensor must take into account the influence of cross-reactivity and cross-talk to the final detection results. To investigate the cross-reactivity and cross-talk between the target antibody and non-cognate antibodies, three control tests were carried out: (1) blank, (2) single antibody, CEA or AFP, and (3) simultaneous detection.

The results of DPV were obtained by comparing the peak currents response of the immunosensor that were incubated in $0.01 \text{ ng}\cdot\text{mL}^{-1}$ AFP or CEA, $0.01 \text{ ng}\cdot\text{mL}^{-1}$ AFP or CEA + $1 \text{ ng}\cdot\text{mL}^{-1}$ CEA or AFP, $5.0 \text{ ng}\cdot\text{mL}^{-1}$ AFP or CEA + $1 \text{ ng}\cdot\text{mL}^{-1}$ CEA or AFP, $5.0 \text{ ng}\cdot\text{mL}^{-1}$ AFP or CEA + $20.0 \text{ ng}\cdot\text{mL}^{-1}$ CEA or AFP and $80.0 \text{ ng}\cdot\text{mL}^{-1}$

AFP + 80.0 ng·mL⁻¹ CEA, respectively. The results showed in Fig.S5. For the 0.01 ng·mL⁻¹ AFP, the immunosensors **have shown** AFP corresponding **peak** current responses, but no CEA **corresponding peak** current response (Fig.S 5A, curve a). After increasing 1 ng·mL⁻¹ CEA, the current response at the immunosensor for CEA emerged, while the immunosensors for AFP did not show change (Fig.S 5A, curve b). The current response of AFP obviously increased, while the current response of CEA almost no change when 5 ng·mL⁻¹ of AFP was added (Fig.S 5A, curve c). The same experiment is performed when CEA and AFP was swapped, the results showed in Fig.S 5B. For the 5.0 ng·mL⁻¹ AFP or CEA + 20 ng·mL⁻¹ CEA or AFP, the immunosensors **shown** AFP and CEA corresponding **peak** current responses (Fig.S 5C, curve a, b), the current response of both AFP and CEA obviously increased for 80 ng·mL⁻¹ AFP and CEA (Fig.S 5C, curve c). The results indicated that no electrochemical cross-talk occurred and the cross-reactivity between the two target antibodies towards non-cognate proteins was negligible in a single run without interfering with each other. Thereby, the two target antibodies immunoassay could be performed in a single run.



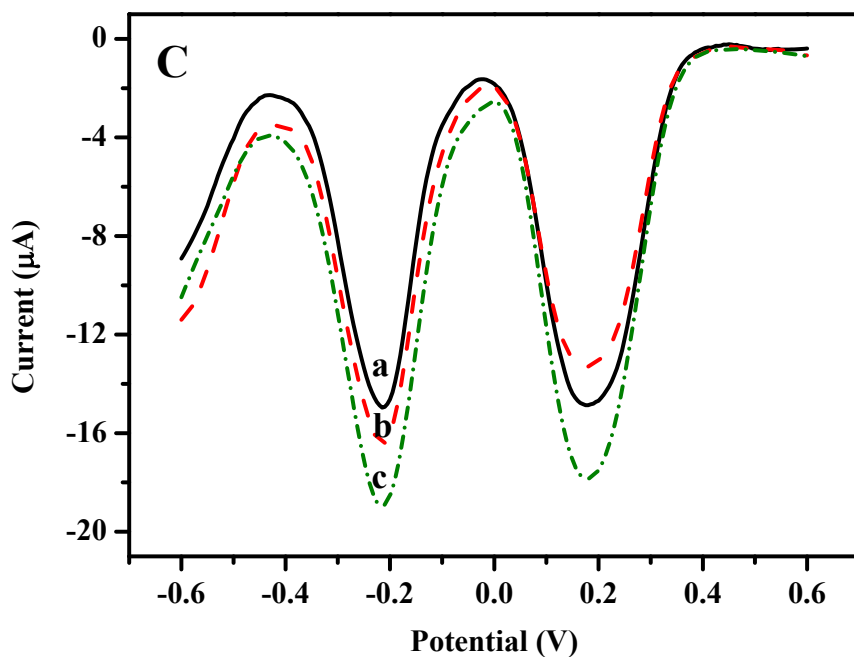
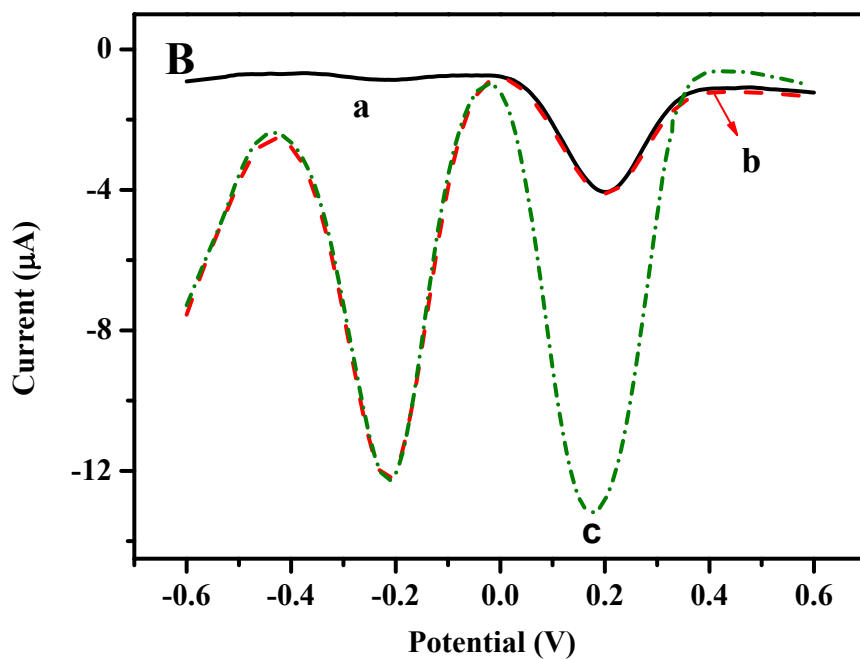


Fig. S5 Cross-reactivity of the array: DPV for $0.01 \text{ ng}\cdot\text{mL}^{-1}$ AFP + $0 \text{ ng}\cdot\text{mL}^{-1}$ CEA (a), $0.01 \text{ ng}\cdot\text{mL}^{-1}$ AFP + $1 \text{ ng}\cdot\text{mL}^{-1}$ CEA (b) and $5 \text{ ng}\cdot\text{mL}^{-1}$ AFP + $1 \text{ ng}\cdot\text{mL}^{-1}$ CEA (c) (A), $0 \text{ ng}\cdot\text{mL}^{-1}$ AFP + $0.01 \text{ ng}\cdot\text{mL}^{-1}$ CEA (a), $1 \text{ ng}\cdot\text{mL}^{-1}$ AFP + $0.01 \text{ ng}\cdot\text{mL}^{-1}$ CEA (b) and $1 \text{ ng}\cdot\text{mL}^{-1}$ AFP + $5 \text{ ng}\cdot\text{mL}^{-1}$ CEA (c) (B), $5 \text{ ng}\cdot\text{mL}^{-1}$ AFP + $20 \text{ ng}\cdot\text{mL}^{-1}$ CEA (a), $20 \text{ ng}\cdot\text{mL}^{-1}$ AFP + $5 \text{ ng}\cdot\text{mL}^{-1}$ CEA (b) and $80 \text{ ng}\cdot\text{mL}^{-1}$ AFP + $80 \text{ ng}\cdot\text{mL}^{-1}$ CEA (c) (C) in $0.1 \text{ M PBS (pH 7.4)} + 0.1 \text{ M KCl}$

1.5 Optimization of experimental parameters

The electrochemical performance of the immunosensor was often related to great quantity factors, such as the pH value of the detection solution, the incubation time and incubation temperature. To obtain the optimum conditions for the detection of AFP and CEA, the above three factors were optimized in $20 \text{ ng}\cdot\text{mL}^{-1}$ AFP and CEA by CV. The effects of pH value of the detection solution on the current responses to AFP and CEA were shown in Fig.S 6A. The current response increased when increasing the pH value from 4.5 to 7.4, and then sharply decreased when the pH values higher than 7.4. Because the pH value of the detection solution could not only influence the activity of the antigens and antibodies, but also the electrochemical behavior of the electron mediator Cu_2O and Fc-COOH . Thus, the pH 7.4 was selected for the detection AFP and CEA.

The incubation time was another important factor in the performance of the immunosensor. When antigens reached the antibodies that were modified on the surface of the electrode, it took some time for the species contact to form immune-complexes. Hence, the effect of incubation time was investigated in Fig.S 6B. The peak current responses to AFP and CEA increased rapidly when increasing the incubation time used in this immunoassay, and then started to level off at 40 min. which showed saturated binding in the immunoreactions. Thus, 40 min was selected as optimal incubation time for the immunoassay. In order to convenience of the experiment operation, the room temperature was selected as the optimal incubation temperature.

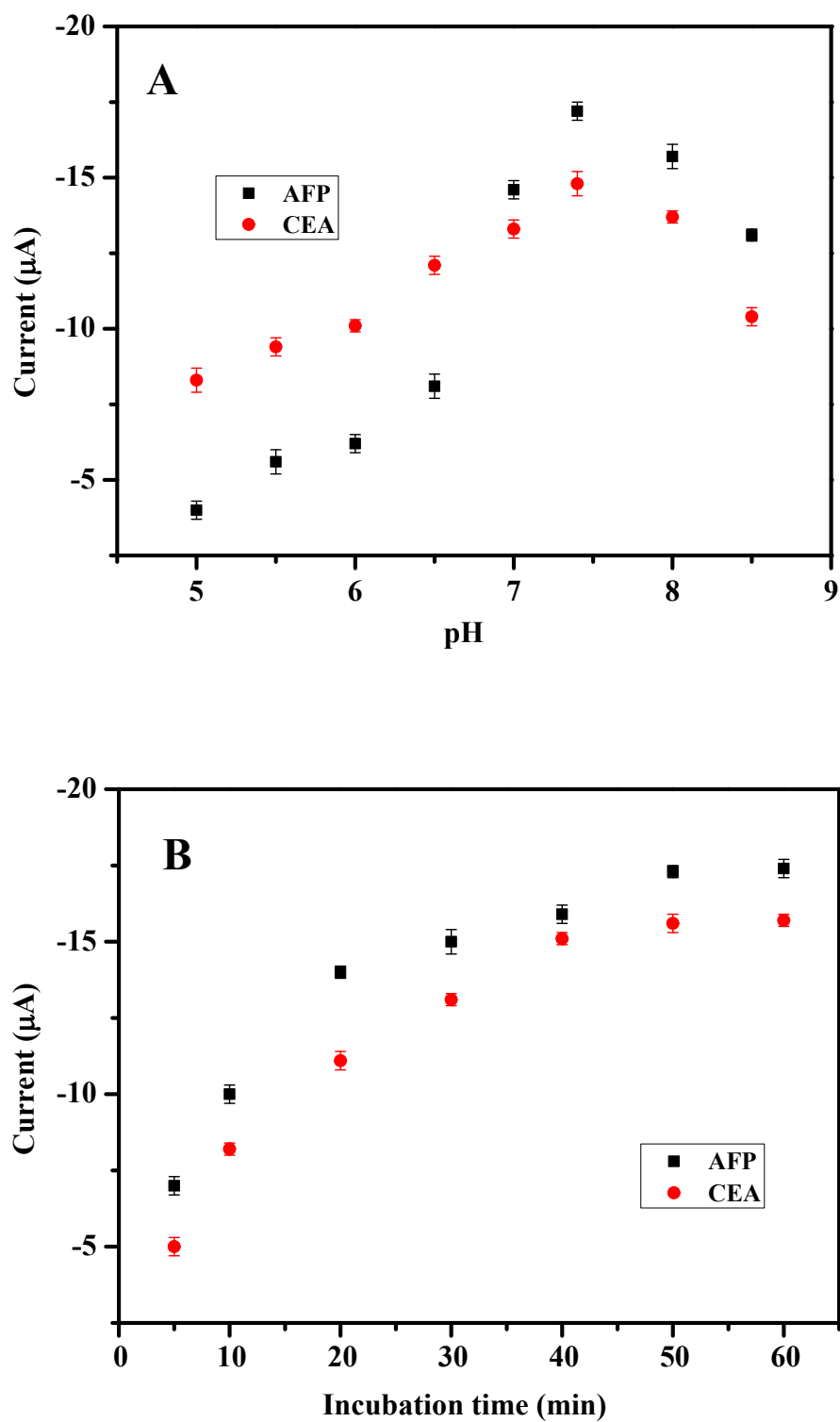


Fig. S6 Effects of pH (A) of detection solution and incubation time (B). Above detections in 0.1 M PBS (pH 7.4) solution containing 0.1 M KCl. Error bar = SD (n=5)

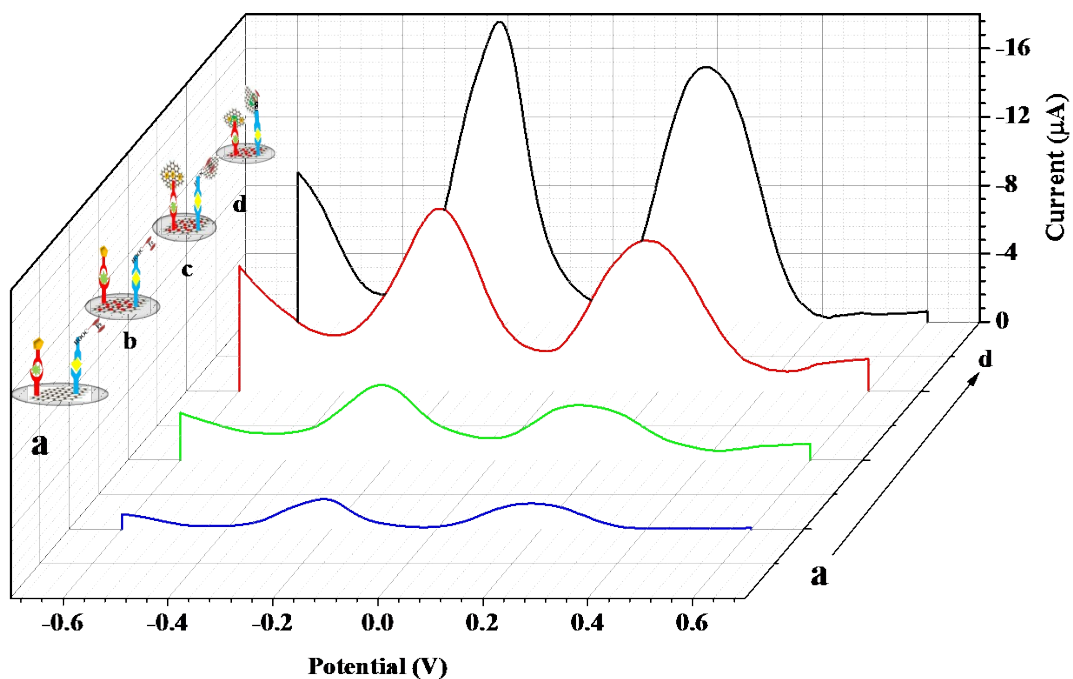


Fig. S7 Electrochemical immune-responses of Cu_2O - or $\text{Fc-Ab}_2/\text{antigen/BSA/Ab}_1/\text{AuNPs/GCE}$ (a), Cu_2O - or $\text{Fc-Ab}_2/\text{antigen/BSA/Ab}_1/\text{GO-AuNPs/GCE}$ (b), $\text{Cu}_2\text{O-GO-}$ or $\text{GO-Fc-Ab}_2/\text{antigen/BSA/Ab}_1/\text{GO-AuNPs/GCE}$ (c), $\text{Cu}_2\text{O-GO-CD-}$ or $\text{GO-Fc-CD-Ab}_2/\text{antigen/BSA/Ab}_1/\text{GO-AuNPs/GCE}$ (d) in 0.1 M PBS (pH 7.4) solution containing 0.1 M KCl under optimal conditions

Table S1 Comparison of analytical properties of different immunoassays toward CEA and AFP

Probes	Linear range		Detection limit		Ref.
	(ng·mL ⁻¹)		(ng·mL ⁻¹)		
	AFP	CEA	AFP	CEA	
Au-TB/Fc-rGO-Ab ₂	0.01-100	0.01-100	0.002	0.003	4
GOD-Au/CNTs-Ab ₂	0.0025-2.5	0.0025-2.0	0.0022	0.0014	5
rGO/PB/Thi/AuNPs-Ab ₂	0.01-300	0.01-300	0.00085	0.00065	6
GT/PMs-Ab ₂	1-80	1-60	0.89	0.6	7
Thi/Fc@Ab ₂ -PtNP-HRP	0.5-50	0.3-45	0.08	0.05	8
CGS-TB/PB-Ab ₂	0.5-60	0.5-60	0.05	0.1	9
PLL-Au-Cd/Pb-Apo-Ab ₂	0.01-50	0.01-50	0.004	0.004	10
PODP/poly(VFc-ATP)-Ab ₂	0.01-100	0.01-100	0.003	0.006	11
β-CD-GO-Fc/Cu ₂ O-Ab ₂	0.001-80	0.001-80	0.0002	0.0001	This work

Table S2 Assay results of clinical serum samples using this immunosensor and ELISA (n=5)

Sample NO.	This immunosensor		ELISA		Relative error	
	(ng·mL ⁻¹) ^a		(ng·mL ⁻¹) ^a		(%)	
	CEA	AFP	CEA	AFP	CEA	AFP
1	0.23	0.76	0.24	0.74	4.2	2.7
2	1.37	4.38	1.41	4.22	2.8	3.8
3	10.46	5.59	10.17	5.74	3.1	2.6
4	5.19	3.25	4.95	3.38	4.8	3.9
5	4.96	6.34	5.11	6.09	2.9	4.1

^a Mean value of five measurements.

References

- 1 W. Hummers, R. J. Offeman, *J. Am. Chem. Soc.*, 1958, **80**, 1339.
- 2 T. Wu, L. Zhang, J. Gao, Y. Liu, C. Gao, J. Yan, *J. Mater. Chem. A*, 2013, **1**, 7384-7390.
- 3 X. Chen, G. Wu, J. Chen, X. Chen, Z. Xie, X. Wang, *J. Am. Chem. Soc.*, 2011, **133**, 3693-3695.
- 4 N. Liu, Z. Liu, H. Han, Z. Ma, *J. Mater. Chem. B*, 2014, **2**, 3292-3298.
- 5 G. Lai, F. Yan, H. Ju, *Anal. Chem.* 2009, **81**, 9730-9736.
- 6 X. Jia, Z. Liu, N. Liu, Z. Ma, *Biosens. Bioelectron.*, 2014, **53**, 160-166.
- 7 Z. Yang, H. Liu, C. Zong, F. Yan, H. Ju, *Anal. Chem.*, 2009, **81**, 5484-5489.
- 8 Z. Song, R. Yuan, Y. Chai, Y. Zhuo, W. Jiang, H. Su, X. Che, J. Li, *Chem. Commun.*, 2010, **46**, 6750-6752.
- 9 X. Chen, X. Jia, J. Han, J. Ma, Z. Ma, *Biosens. Bioelectron.*, 2013, **50**, 356-361.
- 10 D. Wang, T. Li, N. Gan, H. Zhang, N. Long, F. Hu, Y. Cao, Q. Jiang, S. Jiang, *Electrochim. Acta*, 2015, **163**, 238-245.
- 11 Z. Liu, Q. Rong, Z. Ma, H. Han, *Biosens. Bioelectron.*, 2015, **65**, 307-313.